RSC Advances

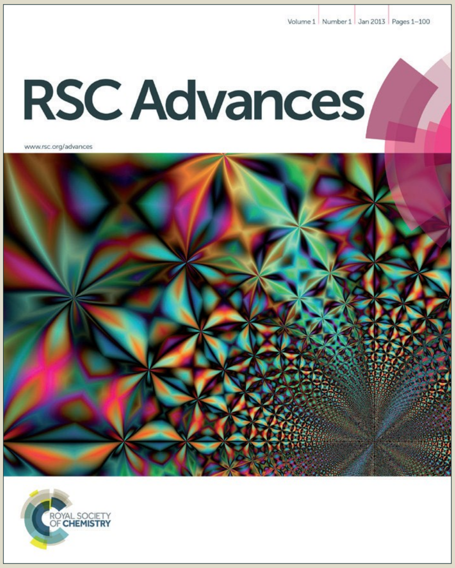

ROYAL SOCIETY
OF **CHEMISTRY**

www.rsc.org/advances

RSC Advances

PAPER

Order-Enhanced Silver Nanowire Networks Fabricated by Two-Step Dip-Coating as Polymer Solar Cell Electrodes

Received 00th January 20xx,
Accepted 00th January 20xx

DOI: 10.1039/x0xx00000x

www.rsc.org/

Danfeng Pu,[a] Weixin Zhou,[a] Yi Li,*[a] Jun Chen,[a] Jianyu Chen,[a] Hongmei Zhang,[a] Baoxiu Mi,[a] Lianhui Wang,[a] Yanwen Ma*[a]

Abstract: The efficient utilization of Ag NW by avoiding their aggregation and multi-layer stacking in their networks can improve the optical and electrical properties of the derived transparent conductive electrodes (TCEs). In this work, we develop a two-step dip-coating process to prepare Ag NW networks on polyethylene terephthalate (PET) substrates using three types of Ag NW with length/diameter (L/D) ratio of 100, 400 and 1000 respectively. The NW with small or medium L/D (100 and 400) are likely to form order-enhanced networks since they are rigid and easy to be separated. The TECs prepared by this approach present much higher performance than those prepared by spray coating. The optimal Ag NW-based TCEs show a typical sheet resistance of 35 Ω sq^{-1} with high transparency of 92%. The polymer solar cells constructed on the resulting TCEs can give an efficiency of 3.28%, demonstrating the potential application of our Ag NW/PET films as the ITO alternative in flexible solar cells.

Introduction

Transparent conductive electrodes (TCEs) are critical components of thin-film optoelectronic devices, such as liquid-crystal displays, light-emitting diodes, solar cells and touch screens.[1-5] Currently, indium tin oxide (ITO) is the most high-performance TCE in use due to its excellent conductivity and high optical transparency.[6] ITO film can have sheet resistance under 20 Ω· sq-1 with transparency of 90% when deposited at a high temperature onto glass. However, some disadvantages such as limited indium resources, high manufacturing costs and fragility have hindered ITO application in low-cost, flexible, lightweight electronics.[7, 8] Moreover, the resistance of ITO will increase to 40-200 Ω· sq-1 when deposited on plastic substrate at a low temperature.[9, 10] Hence recent researches have focused on replacing ITO with alternative materials that can be solution processed and can achieve the performance of ITO on various substrates, including plastics.

In recent years, several nanomaterials represented by carbon nanotubes (CNTs), graphene, Ag and Cu nanowires (NW) have demonstrated promising potential in replacement of ITO because they are printable, flexible and even abundant.[11-17] Among these alternatives, Ag NW TCEs are indicated to own competitively electrical and optical properties to ITO, showing the most commercial interest to date. Ag NW are generally deposited onto glass or plastic substrates by Meyer rod coating, airbrush spraying, filtration or spin coating, forming random NW networks. However, such disordered NW arrangement seems to be problematic for the balance of optical and electrical properties as well as the contact with active layer in device fabrication.[18] To obtain alignment or enhance the order of Ag NW, several promising strategies have been developed, including Langmuir-Blodgett[18], bubble template[19], flow- and evaporation-induced assembly.[20-22] In addition, dip coating is a facile approach that very suitable for large-area and mass production and has been well demonstrated in the preparation of CNT[23] and reduced graphene oxide (rGO)[24] films. Isotropic CNTs or rGO suspended in solution were ordered or partially aligned toward anisotropic phase by capillary force at the contact line of the air-liquid-solid interface. Following this mechanism, herein, we develop a two-step dip-coating process to prepare Ag NW networks on polyethylene terephthalate (PET) substrates as illustrated in Figure 1. Surface-cationization PET substrate is immersed into the prepared Ag NW solution and pulled out at a constant withdrawal velocity by dip coater. During the withdrawal process, a concave shaped meniscus formed at air-liquid-solid triple-phase line, and then Ag NW colloids flow into the meniscus due to capillary force.[24-26] As a result, Ag NW adhere to the substrate and orient parallel to movement direction (Figure 1a). The second dip coating is conducted in a vertical direction to the first time, allowing Ag NW to form perpendicularly crossing networks (Figure 1b). To understand the effect of aspect ratio (length/diameter, L/D) on the alignment of NW, Ag NW with different L/D (100, 400 and 1000) are used as building blocks to prepare TCEs. The ones with small or medium L/D (100 and 400) are tend to form ordering arrangement because of their well dispersion and rigid features that can avoid aggregation during assembly. The optimal Ag NW TCFs are obtained on L/D of 400, whose typical sheet resistance (R_S) is 35 Ω· sq^{-1} at high transparency (T) of 92% (λ = 550 nm), superior to that fabricated by spray coating (R_S = 40 Ω·sq^{-1}, T = 87%). The optimal TCEs have been successfully used to

---

[a] Key Laboratory for Organic Electronics and Information Displays & Institute of Advanced Materials (IAM), Jiangsu National Synergistic Innovation Center for Advanced Materials (SICAM), Nanjing University of Posts & Telecommunications, 9 Wenyuan Road, Nanjing 210023, China. E-mail: iamyli@njupt.edu.cn; iamywma@njupt.edu.cn; Tel: (+86) 25-85866353; Fax: (+86) 25-85866396.

† Electronic Supplementary Information (ESI) available: See DOI: 10.1039/x0xx00000x

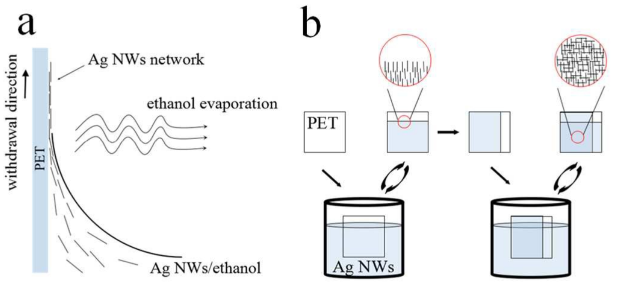

Figure 1. a) Schematic illustration of nanowire assembly in the dip-coating process. b) Two-step dip-coating process.

fabricate polymer solar cells, with an efficiency of 3.28%, which is better than those of the devices using random Ag NW networks and ITO electrodes, demonstrating their potential application as the ITO alternative in flexible solar cells.

Experiment section

Synthesis of Ag NW

Low L/D Ag NW were synthesized by modified polyol reduction approach and medium and high L/D Ag NW were synthesized by hydrothermal process.

In polyol reduction synthesis, 1.6 g $AgNO_3$ was added into 500 mL of glycerol solution containing 5.6 g of PVP after the solution heated to 210 °C. Then, 10 mL of glycerol containing 0.15 g NaCl was added into the system. The reaction was kept for 0.5 h at 210 °C and then cooled down to room temperature naturally. The water was added into the suspension, and the product was obtained by centrifugation and rinsing. The length of the obtained Ag NW is about 5 μm and the diameter is about 50 nm (Supporting Information, Figure S1a & b). The as-prepared Ag NW were dispersed in ethanol for storage.

In hydrothermal process, 0.5 mL $AgNO_3$ (0.1 M) aqueous solution was added into 35 mL aqueous solution containing 0.5 g of glucose and 0.1 g of PVP under vigorously stirring. The mixture was transferred into a 40 mL Teflon-sealed autoclave and heated at 180 □ for 2 or 3 h. After the reaction, the autoclave was allowed to cool in air, and the product was obtained by centrifugation and rinsing. The lengths of the obtained Ag NW samples prepared under 2 and 3 h are about 20 and 50 μm, respectively, and the diameters are about 50 nm (Supporting Information, Figure S1c-f).

Preparation of Ag NW films

PET substrates were modified by immersing in a PDDA solution (1 mg/mL) for 5 minutes and then dried with N_2 gas flow.[27] The substrates were dipped into the Ag NW dispersion (0.1 mg/ml) and withdrawn using a mechanical motor with programmable pulling speeds (1 cm/s). The density of Ag NW on PET substrate was tuned the content of NW in dispersion from 0.1 to 1.0 mg/ml. After one-direction coating, the films were dried in air and then the substrates were tuned vertically to conduct the second-step dip coating. The obtained Ag NW films were annealed at 80 °C for 5 h and pressed at 20 MPa for 10 s. These films are denoted as dc-Ag NW/PET. For comparison, Ag NW/PET films with random networks (denoted as r-Ag NW/PET) were prepared by the spray coating as described in our previous work. [15]

Characterization

Ag NW and their derived films were characterized by scanning electron microscopy (SEM, Hitachi S-4800), transmission electron microscopy (TEM, Hitachi 7700 operated at 120 kV) and optical microscopy (Nikon Instrument Inc. ECLIPSE LV100N POL). The transparency of each film was measured using a UV-vis spectrophotometer (Shimadzu, UV-3600) and the sheet resistance (RS) was evaluated by four-point probe measurement (Keithley 2400 Semiconductor Parameter Analyzer) at room temperature.

Fabrication of polymer solar cells

The optimal dc-Ag NW/PET TCEs with RS = 35 $\Omega\cdot sq^{-1}$ and T = 92%, r-Ag NW/PET with RS = 40 $\Omega\cdot sq^{-1}$ and T = 87% and commercial ITO/glass electrodes (RS = 15 $\Omega\cdot sq^{-1}$ and T = 88%) were used as anodes to construct polymer solar cells. Ag NW-based electrodes were directly used without any treatment, while ITO/glass was exposed to oxygen plasma for 50 s before following coating. PEDOT:PSS with a thickness of approximately 40 nm was spin-coated onto the two type of electrodes. Poly(3-hexylthiophene) (P3HT):phenyl-C61-butyric acid methyl ester (PCBM) with 1:1 weight ratio dissolved in 1,2-dichlorobenzene were used as active materials and spin-coated on the PEDOT:PSS film at 800 rpm for 20 s. The thickness of the active layer was about 90 nm. An aluminum metal cathode was deposited on top by thermal evaporation. The photovoltaic performance was measured under an air mass of a 1.5 solar illumination at 100 $mW\cdot cm^{-2}$ (1sun). Incident photon to current efficiency (IPCE) tests were carried out on a QE/IPCE test system (CROWNTECHCTTH-150W). Impedances of devices were measured with 300 mV amplitude of ac signal at open-circuit potential (Wayne Kerr, WK6500B).

Results discussion

Figure 2a shows the photograph of Ag NW (L/D = 100) film by two-step dip-coating process. Since a margin with 0.5-1 cm was left for clamping during each coating, a cross boundary line was generated between the first and second coating area. The Ag NW film within interlaced area presents homogeneous light transmission, indicating uniform Ag NW networks are prepared. The optical microscopy images of the margins can reflect the distribution of Ag NW in each coating process (Figure 2b and c). It is clearly seen that, Ag NW in these area likely orient to the movement direction. In the overlapping area, Ag NW cross together and from uniform networks. Similar result also can be observed on the Ag NW (L/D = 400) film. The order of Ag NW is significantly enhanced in comparison with the film fabricated by spray coating (Figure S2). However, when the L/D increases to 1000, Ag NW could not be aligned by two-step dip coating. These high-aspect-ratio NW are much flexible and aggregated into bundles by capillary condensation during assembly, especially in the repeated coating because their adhesion to substrate is reduced by the isolation of the pre-deposited NW

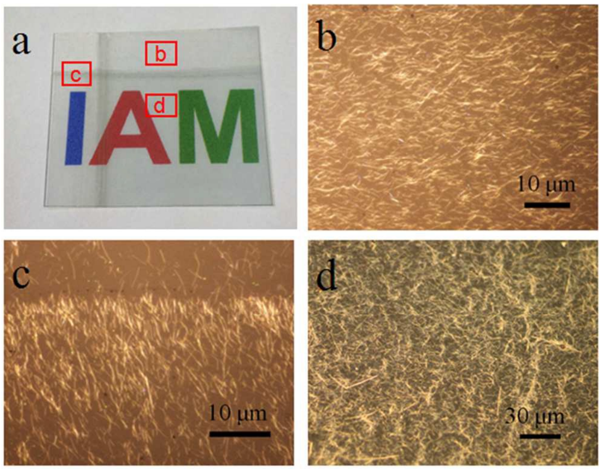

Figure 2. (a) Photograph of dc-Ag NW/PET; (b-c) Optical microscopy images of Ag NW films at margins of first (b) and second coating (c) as well as overlapping area.

(Figure S3). These results suggest that Ag NW with small L/D are much suitable for dip-coating manufacturing than those with large L/D. On the other hand, high aspect ratio of Ag NW is necessary for preparation of high-performance TCEs. Hence we need optimize the aspect ratio of Ag NW when two-step dip coating approach is applied.

Optical microscopy is an efficient method to characterize Ag NW films and could give a large-area vision. But limited by its resolution and focal plane, the detail of NW overlap is not given. Fortunately, SEM can provide an insight of local area for the films. Figure 3 presents the typical SEM images of Ag NW/PET using NW with L/D of 100 and 400 respectively. After the one-step coating, most of NW were arranged in a same direction (Figure 3a and c). The two-step coated NW lay on the pre-deposited NW, forming crossing network (Figure 3b and d). The enlarged images show that these two batches of NW on each film are not strictly perpendicular to each other. The main reason is that the NW are likely to slide on the smooth surface of existed cylindrical NW (Figure S4). The SEM observation well support the optical microscopy result, demonstrating that the order of Ag NW on PET substrates could be enhanced by a facile two-step dip coating process.

The optimal and electrical properties of Ag NW networks prepared from L/D=100 and L/D = 400 Ag NW were tuned by changing the NW content in dispersion. The *T* of dc-Ag NW/PET films was plotted with respect to the R_S, as shown in Figure 4. For comparison, the data of random Ag NW networks, measured from spraying-deposited films, i.e., r-Ag NW/PET and calculated by theoretical simulation by Winey et al., are also plotted in Figure 4. For random Ag NW, the experimental results are well consistent with theoretical simulations. When the films are prepared by two-step dip coating, their performance is significantly elevated. For examples, using L/D = 400 Ag NW, the r-Ag NW/PET films give an optimal R_S of 40 $\Omega\cdot sq^{-1}$ with T = 87% while dc-Ag NW/PET films can decrease R_S to 35 $\Omega\cdot sq^{-1}$ at T = 92%. Moreover, dc-Ag NW/PET films prepared from L/D = 400 NW even have a higher quality than the simulated random networks of L/D = 600 NW.[28] As known, to achieve a Ag NW film with small resistance but high optical transmittance, the NW networks should have a shortest electron transport channel while maximum photon transport area. Compared with randomly distributed NW networks, the order-enhanced ones could reduce the stacking of NW and utilize them more efficiently, allowing the improvement of optimal and electrical properties.

To further investigate the performance of the as-prepared TCEs, bulk heterojunction photovoltaic cells using P_3HT:PCBM were fabricated on optimal dc-Ag NW/PET (R_S = 35 $\Omega\cdot sq^{-1}$, T = 92%) according to the procedure described in the experimental section. For comparison, we also fabricated the same structure device on r-Ag NW/PET (R_S = 40 $\Omega\cdot sq^{-1}$, T = 87%) and ITO/glass (R_S = 15 $\Omega\cdot sq^{-1}$, T = 88%) TCEs. The typical current density-voltage (J-V) curves of these solar cells under both illumination and in the dark are shown

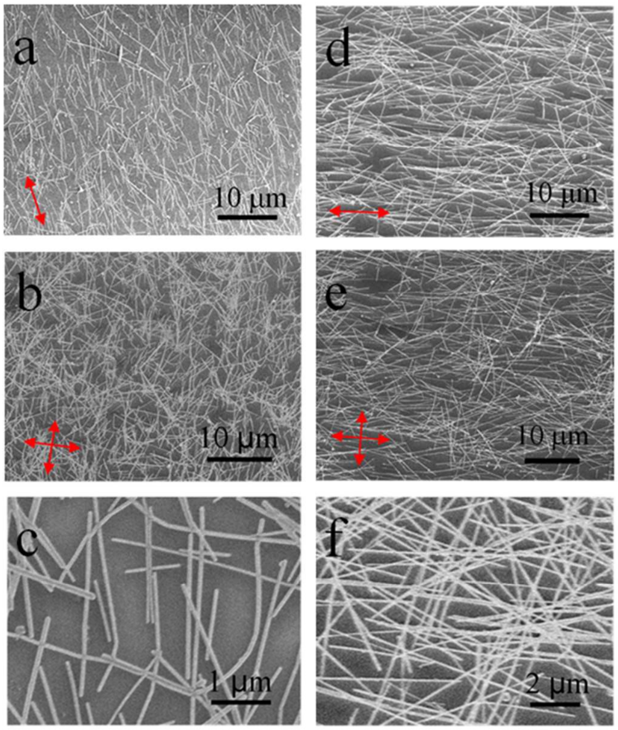

Figure 3. SEM images of dc-Ag NW/PET using NW with L/D of 100 and 400. (a-c) L/D = 100；(d-f) L/D = 400.

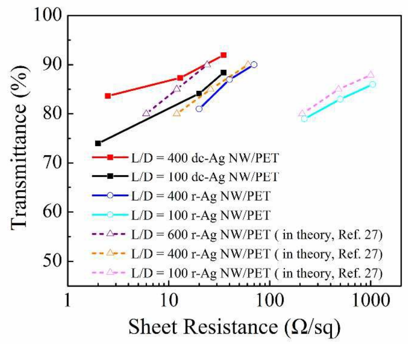

Figure 4. Sheet resistance versus optical transmission (at 550 nm) for dc-Ag NW/PET films, r-Ag NW/PET films and theoretical simulation [28, 29]

in Figure 5a. The r-Ag NW/PET device has a power conversion efficiency (PCE) of 2.83%，a short-circuit current density (J_{SC}) of 9.45 mA·cm^{-2}, an open-circuit voltage (V_{OC}) of 0.58 V, and a fill factor (FF) of 51%. By contrast, the dc-Ag NW/PET device shows a better performance. Its PCE can reach to 3.28 % with J_{SC} = 10.95 mA·cm^{-2}, V_{OC} =0.58 V, and FF =52 %, even higher than the performance of the device on ITO/glass (PCE = 2.95 %, J_{SC} = 9.79 mA·cm^{-2}, V_{OC} = 0.58 V, FF = 52 %). The adsorption and external quantum efficiency (EQE) of these devices are depicted in Figure 5b. The devices using order-enhanced Ag NW networks reveal a sequential increase over the entire visible solar spectrum range in comparison with those on r-Ag NW/PET and ITO/glass, which is consistent with the improved performance of EQE. The increased absorbance can be contributed to the improved transparency. The impedance spectra of the devices demonstrates that dc-Ag NW based devices have lower charge transfer resistance and the time constant than ITO based devices, resulting in the faster charge transfer, and then higher power conversion efficiency.[30] From above results, it demonstrates that these Ag NW networks TCEs preparing by two-step dip-coating approach can be considered as a promising candidate for replacing ITO in the low-cost, high performance and flexible solar cells.

Conclusions

In summary, we have presented a two-step dip-coating approach to prepared order-enhanced Ag NW networks on PET plastic substrate. The Ag NW with small or medium L/D (e.g., 100 and 400) were likely to be aligned due to their rigid features while the ones with large L/D of 1000 were flexible and tend to aggregation in assembly process. The TCEs prepared by two-step dip coating using L/D = 400 Ag NW showed a typical RS of 35 Ω·sq^{-1} at T of 92%, much higher than random Ag NW networks prepared by spray coating (RS = 40 Ω· sq^{-1} and T = 87%). The outstanding optical and electrical properties owned by the resulting Ag NW/PET allow them to demonstrate high performance in polymer solar cell device. The power conversion efficiency of the device reached to 3.28 %, even spurious to that of device on ITO electrodes. As the two-step dip-coating approach is facile and competent for large-scale production, we expect it can provide the clue to improve the quality of Ag NW-based TCEs for future application in flexible electronic devices.

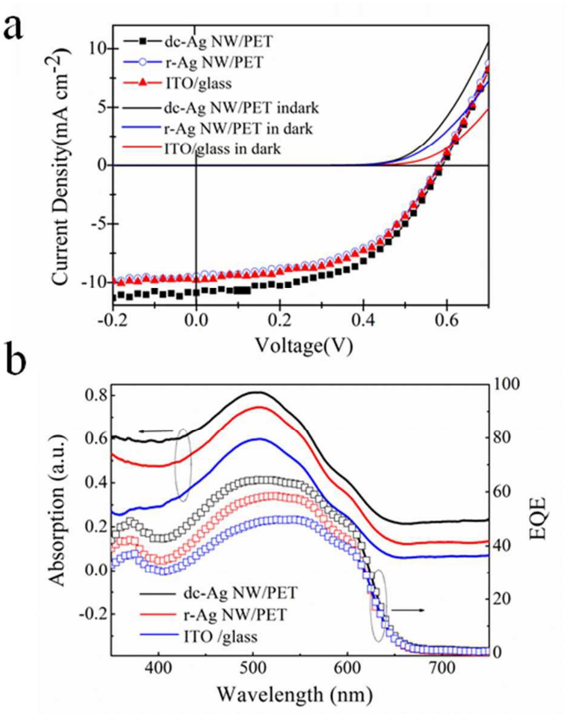

Figure 5. (a) Current density–voltage (J–V) characteristics in the dark and under simulated AM 1.5 solar irradiation with 100 mW·cm^{-2} intensity for devices on dc-Ag NW/PET, r-Ag NW/PET and ITO/glass electrdes; (b) Absorption and EQE.

Acknowledgements

This work is jointly supported by NSFC (61504062), Priority Academic Program Development of Jiangsu Higher Education Institutions (YX03001), Jiangsu National Synergetic Innovation Center for Advanced Materials (SICAM), Synergistic Innovation Center for Organic Electronics and Information Displays, Jiangsu Provincial NSF (BK20141424, BK20150863), Qing Lan Project of Jiangsu Province, and Scientific Research Foundation of NUPT (NY214183).

References

1 M. Layani, A. Kamyshny and S. Magdassi, *Nanoscale*, 2014, **6**, 5581.
2 M. Song, D. S. You, K. Lim, S. Park, S. Jung, C. S. Kim, D.-H. Kim, D.-G. Kim, J.-K. Kim, J. Park, Y.-C. Kang, J. Heo, S.-H. Jin, J. H. Park and J.-W. Kang, *Adv. Funct. Mater.*, 2013, **23**, 4177.
3 E.-C. Cho, C.-P. Li, J.-H. Huang, K.-C. Lee and J.-H. Huang, *ACS Appl. Mater. Interfaces,* 2015, **7**, 11668.
4 X. Guo, X. Liu, F. Lin, H. Li, Y. Fan and N. Zhang, *Sci. Rep.*, 2015, **5**, 10569.
5 A. R. Madaria, A. Kumar and C. Zhou, *Nanotechnology*, 2011, **22**, 245201
6 R. B. H. Tahar, T. Ban, Y. Ohya and Y. Takahashi, *J. Appl. Phys.*, 1998, **83**, 2631.
7 S. Ye, A. R. Rathmell, Z. Chen, I. E. Stewart and B. J. Wiley, *Adv. Mater*., 2014, **26**, 6670.
8 D. R. Cairns, R. P. Witte, D. K. Sparacin, S. M. Sachsman, D. C. Paine and G. P. Crawford, *Appl. Phys. Lett*., 2000, **76**, 1425.
9 B. G. Lewis and D. C. Paine, *MRS Bull*., 2000, **25**, 22.
10 B. L. Gehman, S. Jonsson, T. Rudolph, M. Scherer, M. Weigert and R. Werner, *Thin Solid Films*, 1992, **220**, 333.
11 D. S. Hecht, L. Hu and G. Irvin, *Adv. Mater*., 2011, **23**, 1482.
12 A. R. B. M. Yusoff, D. Kim, F. K. Schneider, W. J. da Silva and J. Jang, *Energy Environ. Sci*., 2015, **8**, 1523.
13 T. Y. Kim, Y. W. Kim, H. S. Lee, H. Kim, W. S. Yang and K. S. Suh, *Adv. Funct. Mater*., 2013, **23**, 1250.
14 L. Yang, T. Zhang, H. Zhou, S. C. Price, B. J. Wiley and W. You, *ACS Appl. Mater. Interfaces*, 2011, **3**, 4075.
15 J. Chen, W. Zhou, J. Chen, Y. Fan, Z. Zhang, Z. Huang, X. Feng, B. Mi, Y. Ma and W. Huang, *Nano Res.*, 2015, **8**, 1017.
16 J. Song, J. Li, J. Xu and H. Zeng. *Nano Lett*., 2014, **14** , 6298.
17 H. Z. Guo, N. Lin, Y. Z. Chen, Z. W. Wang, Q. S. Xie, T. C. Zheng, N. Gao, S. P. Li, J. Y. Kang, D. J. Cai and D.-L. Peng, *Sci. Rep*., 2013, **3**, 2323.

18 J.-W. Liu, J.-L. Wang, Z.-H. Wang, W.-R. Huang and S.-H. Yu, *Angew. Chem. Int. Ed.*, 2014, **53**, 13477.
19 T. Tokuno, M. Nogi, J.T. Jiu, T. Sugahara and K. Suganuma, *Langmuir*, 2012, **28**, 9298.
20 A. Tao, F. Kim, C. Hess, J. Goldberger, R. R. He, Y. G. Sun, Y. N. Xia and P. D. Yang, *Nano Lett.*, 2003, **3**, 1229.
21 J. W. Liu, J. L. Wang, W. R. Huang, L. Yu, X. F. Ren, W. C. Wen and S. H. Yu, *Sci. Rep.*, 2012, **2**, 987.
22 H. Dai, R. Q. Ding, M. C. Li, J. J. Huang, Y. F. Li and M. Trevor, *Sci. Rep.*, 2014, **4**, 6742.
23 T. A. Shastry, J. W. T. Seo, J. J. Lopez, H. N. Arnold, J. Z. Kelter, V. K. Sangwan, L. J. Lauhon, T. J. Marks and M. C. Hersam, *Small*, 2013, **9**, 45.
24 R. Tkacz, R. Oldenbourg, A. Fulcher, M. Miansari and M. Majumder, *J. Phys. Chem. C*, 2014, **118**, 259.
25 E. Y. Jang, T. J. Kang, H. W. Im, D. W. Kim and Y. H. Kim. *Small*, 2008, **4**, 2255.
26 J. Huang, R. Fan, S. Connor, P. Yang, *Angew. Chem. Int. Ed.*, 2007, **46**, 2414.
27 Y. Li, P. Cui, L. Y. Wang, H. Lee, K. Lee and H. Lee, *ACS Appl. Mater. Interfaces.*, 2013, **5**, 9155.
28 R. M. Mutiso, M. C. Sherrott, A. R. Rathmell, B. J. Wiley and K. I. Winey, *ACS Nano*, 2013, **7** , 7654.
29 S. M. Bergin, Y.-H. Chen, A. R. Rathmell, P. Charbonneau, Z.-Y. Li and B. J. Wiley, *Nanoscale*, 2012, **4**, 1996.
30 G.-H. Kim, H.-K. Song, J. Y. Kim, *Energy Mater. Sol. Cells*, 2011, **95**, 1119.